

# Self-organization of silica nano-particles induced by the ion beam

Stjepan Lugomer<sup>1</sup>, Zsolt Zolnai<sup>\*,2</sup>, Attila L. Tóth<sup>2</sup>, and István Bársony<sup>2</sup>

<sup>1</sup> Rudjer Boskovic Institute, Bijenicka c. 54, 10001, Zagreb, Croatia

<sup>2</sup> Research Institute for Technical Physics and Materials Science (MTA MFA), P.O.B. 49, 1525 Budapest, Hungary

Received 3 October 2010, accepted 4 February 2011

Published online 31 May 2011

**Keywords** nanoparticles, Langmuir-Blodgett layer, ion irradiation, self-organization

\* Corresponding author: e-mail zolnai@mfa.kfki.hu, Phone: (+36-1) 392 2222/3661, Fax: (+36-1) 392 2235

We studied the self-organization (SO) of small-size ( $D = 90$  nm), medium-size (220 nm), and large-size (450 nm) colloidal silica nanoparticles in Langmuir-Blodgett layers induced by a focused  $\text{Ga}^+$  ion beam with energy of 30 keV. The ion irradiation induces SO into various types of clusters as the result of particle charging and heating, Coulomb repulsion and motion on the substrate surface, as well as of particle - particle and particle - substrate interaction. These processes show a great difference of the underlying dynamics and of the charac-

teristics of SO pattern, depending on the particle size and on the ion fluence. The two dimensional (2D) pattern of the small-size particles is transformed into “infinite” chain-cluster, while the pattern of medium-size particles is transformed into a number of short separated chain-clusters. The pattern of large-size particles is mostly unchanged, but shows particle melting and buckling, which at higher fluences passes into ion beam-induced sputtering.

© 2011 WILEY-VCH Verlag GmbH & Co. KGaA, Weinheim

**1 Introduction** Recent modern topics of nanoscience and nanotechnology relate to the hexagonally ordered mono- and multi-layers of silica nanoparticles, which can be considered as tunable photonic crystals [1, 2], or nano-masks used for modification of the local optical, electrical, or magnetic properties of macroscopic surfaces at the nanoscale by low energy ion bombardment [3]. Beyond surface patterning, these nanofabrication processes are basically related to the SO of the silica monolayer due to ion-particle and particle-particle interactions.

Motivation for this study was to shed more light on the SO of the LB layer of nanoparticles induced by a low energy focused ion beam, and its dependence on the nanoparticle size and on the ion fluence.

We show that induced SO of silica particles is associated with their charging, Coulomb repulsion and motion, heating/surface melting, and discharging, taking place in the particle-particle and particle-substrate adhesive interaction, and causing their reorganization into chain-like clusters.

The results obtained clarify the particle dynamics under low energy ion irradiation, showing that the self-organization occurs by the symmetry breaking of the 2D

regular or irregular lattice, without spherical particle deformation. They are complementary to the results of the particle shaping effect observed in the high ion energy range, in which the pattern transformation occurs by the spherical particle deformation into ellipsoidal or hexagonal ones without 2D lattice symmetry breaking, as reported by Zolnai *et al* at  $E = 500$  keV [4], T. van Dillen *et al.* [1, 5, 6] and Snoeks *et al.* at 4 MeV [7, 8], J. C. Cheang-Wong *et al* at 8 MeV [9], and by Skupinski *et al* at 25 MeV [10] ion energy, respectively.

## 2 Experimental

The colloidal Stöber silica nanospheres of the size  $D = 90$ , 220 and 450 nm in diameter were deposited on (100) silicon substrates by the Langmuir-Blodgett technique [4, 11]. The low energy (30 keV) scanning  $\text{Ga}^+$  ion beam, as a commonly applied nanofabrication tool, has been used to irradiate the LB monolayers of silica particles in rectangular windows with areas ranging from 2.25 to 25  $\mu\text{m}^2$ . The ion beam current has been varied in the range 8 pA – 700 pA for the different window sizes. The irradiation was performed by the Focused Ion Beam (FIB) col-

umn of a LEO 1540XB cross beam FESEM-FIB system. After the ion bombardment Field Emission Scanning Electron Microscopy (FESEM) has been used to monitor the reorganization of the silica nanoparticles.

**3 Results** The as-formed LB layer of silica nanoparticles, self-organized into quasi-regular or regular face-centered hexagonal (*fch*) cells, after irradiation by the ion beam shows a variety of reorganized patterns as a result of dynamics which depends on both the particle size and the ion fluence.

The layer of small-size particles ( $D = 90$  nm) irradiated by the ion beam at the fluence of  $1.1 \times 10^{16} \text{ Ga}^+/\text{cm}^2$  becomes restructured into connected clusters, see Fig. 1(a) (top left), the characteristics of which is also shown at higher magnification (bottom left). Increasing the ion fluence to  $2.2 \times 10^{16} \text{ Ga}^+/\text{cm}^2$ , the particles form a single irregular cluster which extends over the whole spot, representing virtually an “infinite” chain-cluster. Increasing further the fluence to  $4.4 \times 10^{16} \text{ Ga}^+/\text{cm}^2$ , the characteristics of the chain-cluster change only slightly showing the onset of surface melting and coalescence of silica particles (bottom right). The structural analysis reveals that chain segments do not comprise remnants of the initial *fch* cellular structure, indicating the formation of chains by Brownian motion and aggregation.

The LB layer of medium-size silica particles ( $D = 220$  nm), irradiated by the ion beam at the fluence of  $7.8 \times 10^{16} \text{ Ga}^+/\text{cm}^2$ , becomes restructured into small clusters, see Fig. 1(b) (top left). Larger magnification reveals that these un-connected (separated) clusters comprise some characteristics of the former cellular lattice arrangement (bottom left). Increasing the fluence to  $1.6 \times 10^{17}$ , and to  $2.4 \times 10^{17} \text{ Ga}^+/\text{cm}^2$ , the small clusters become reorganized into short unconnected chains (top and bottom right). The structural analysis indicates their formation by decomposition of the *fch* cells, caused by the angular motion and unfolding of its ark-like segments. In contrast to the “infinite” chain of small particles, these short ones have not been formed by the Brownian motion.

The LB layer of large-size silica particles ( $D = 450$  nm), irradiated by the ion beam at the fluence of  $9 \times 10^{16} \text{ Ga}^+/\text{cm}^2$ , becomes only slightly restructured or not restructured at all, see Fig. 1(c) (top left). Larger magnification reveals only slight disturbance and fluctuation of particles around their original position (bottom left). Further increase of fluence to  $3.6 \times 10^{17} \text{ Ga}^+/\text{cm}^2$  causes significant melting and buckling of spherical particles into cylindrical ones with hemispherical top surface (top right). At the fluence of  $7.9 \times 10^{17} \text{ Ga}^+/\text{cm}^2$  due to strong ion beam-induced sputtering the particles vanish leaving only narrow pillars at their previous positions, see Fig. 1(c) (bottom right). The pattern of pillars does not indicate appreciable motion of the particles from their original place.

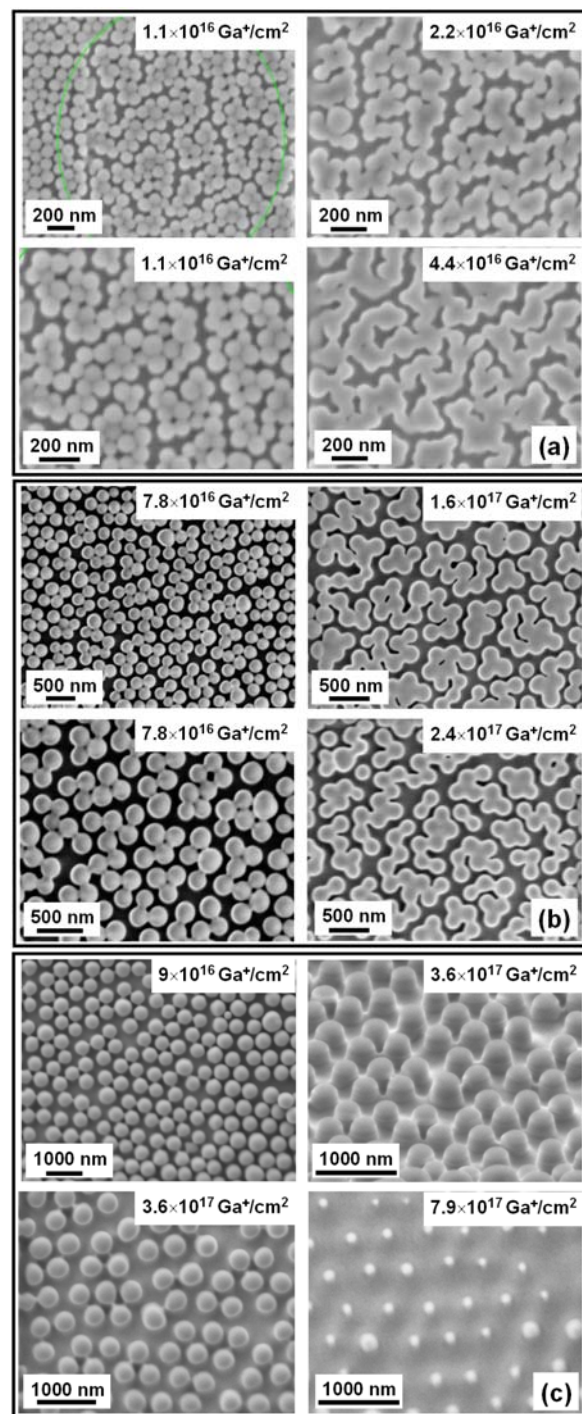


**Figure 1** Self-organization of silica nanoparticles induced by the ion beam. (a)  $D = 90$  nm; Hexagonal layer restructured into connected clusters (top left); Infinite chain-cluster (bottom left); Melting and coalescence of particles in the chain-cluster (top and bottom right); (b)  $D = 220$  nm; Hexagonal layer restructured into isolated clusters (top left); Characteristics of chain-clusters (bottom left); Short chain-clusters (top and bottom right); (c)  $D = 450$  nm; Disturbed hexagonal layer (top left); Characteristic of disturbed layer (bottom left); Buckling of particles (side view, top right); Sputtering of particles (top view, bottom right).

## 4 Discussion

**4.1 Particle charging, Coulomb repulsion, and motion** The ion beam-induced generation of holes [12] and charging of silica causes the Coulomb repulsive force ( $F_C$ ) acting between the nanoparticles. The value of  $F_C$  between two neighboring particles was calculated as function of the ion fluence for various particle sizes, the results are shown in Fig. 2(a). The calculation of charge accumulation is based on a previous experiment of Yogeve *et al.* [12] where the surface potential change induced by the focused  $\text{Ga}^+$  ion beam was measured with Kelvin probe microscopy on planar silica layers.

Following Yogeve's interpretation, the Coulomb force between two particles reaches saturation for the fluence of  $\sim 10^{14}/\text{cm}^2$  staying almost unchanged up to  $\sim 10^{16}/\text{cm}^2$ . Beyond this fluence, the Coulomb force starts to decrease with increasing fluence and eventually vanishes above  $\sim 10^{18}/\text{cm}^2$ , see Fig. 2(a). Sudden increase of the generation rate of shallow traps (dangling bonds) which capture holes, as well as sputtering induced surface erosion reduces the charge [12], and decreases the Coulomb force between the particles.

The pattern reorganization starts once the Coulomb repulsive force reaches the threshold required to push-off and rolling of particles on the substrate. The *threshold Coulomb force*,  $F_{\text{threshold}}$  - should overcome the friction force  $F_{\text{FR}}$  of the solid sphere on the Si surface:

$$F_{\text{threshold}} \geq F_{\text{FR}} \quad (1)$$

The friction force is given by [13]:

$$F_{\text{FR}} = \tau S \quad (2)$$

where  $\tau$  is the interfacial shear strength (representing the friction force per unit area of materials), and  $S$  is the interfacial contact area. The silica/Si interfacial contact area is given by  $S = a^2 p$ , where  $a$ , the contact radius of the circular contact area, is calculated as [13]:

$$a = \left( 2\pi\gamma \left( R^2 / K \right) \right)^{1/3} \quad (3)$$

Here  $\gamma = 0.4 \text{ J/m}^2$  is the Dupré energy of adhesion, or work of adhesion,  $R$  is the radius of the spherical particle, and  $K = 78 \text{ MPa}$  is the reduced Young modulus of the silica/Si system [13], respectively. The above equations result in friction forces of  $F_1 \sim 6 \text{ nN}$ ,  $F_2 \sim 11 \text{ nN}$ , and  $F_3 \sim 17 \text{ nN}$ , which are the threshold Coulomb forces for silica particles of  $D = 90 \text{ nm}$ ,  $220 \text{ nm}$ , and  $450 \text{ nm}$ , respectively. In Fig. 2(a) these threshold forces are marked with horizontal lines. One can see that for each particle size the ion beam induced Coulomb force exceeds the corresponding threshold force, therefore the rolling of particles on the silicon surface can occur.

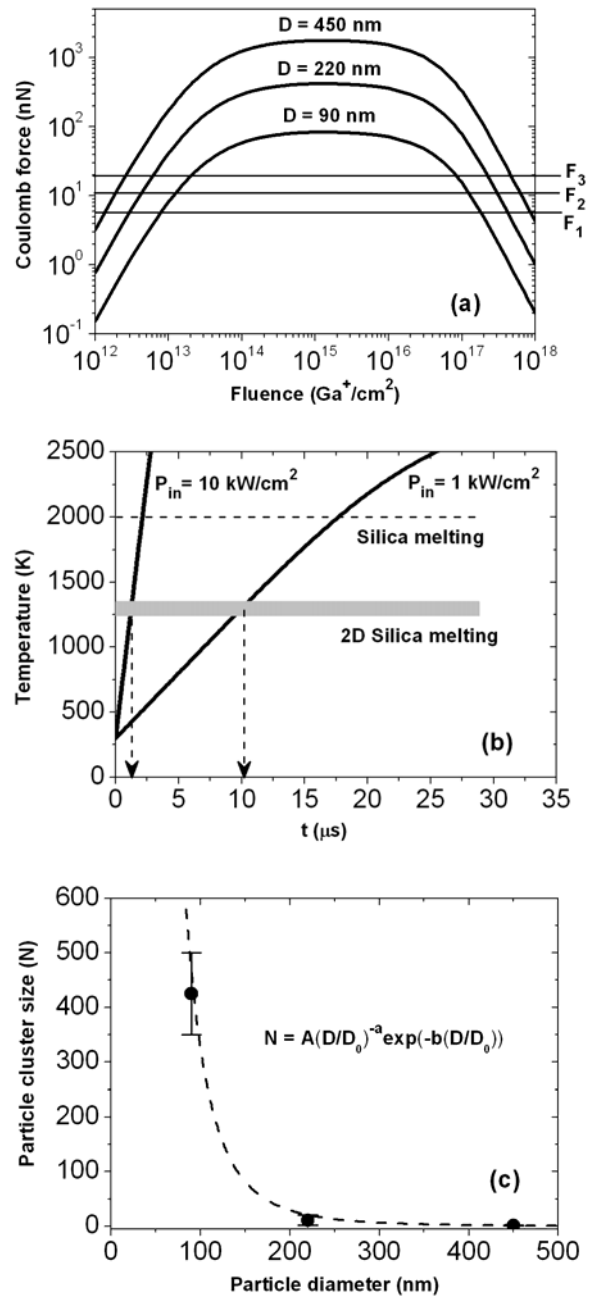


**Figure 2** (a) Coulomb force vs  $\text{Ga}^+$  ion fluence for  $D = 90$ ,  $220$  and  $450 \text{ nm}$  particles.  $F_1$ ,  $F_2$ , and  $F_3$  represent the corresponding threshold forces for the motion of particles due to Coulomb repulsion. (b) Heating of silica nanoparticles by input powers of  $P_{\text{in}} = 10 \text{ kW/cm}^2$  and  $1 \text{ kW/cm}^2$ ; the temperature of 2D surface melting of silica,  $\Theta \geq 1200 \text{ K}$  is reached within  $\sim 1 \mu\text{s}$  and  $10 \mu\text{s}$ , respectively. (c) Cluster-size distribution as function of particle diameter.



**4.2 Particle heating** The high local ion flux of  $\Phi \sim 10^{18}/\text{cm}^2\text{s}$  accompanied by an estimated input power density range of  $P_m = 1\text{--}10\text{ kW}/\text{cm}^2$  causes the fast heating of the particles so that the temperature of 2D surface melting of silica,  $\Theta \geq 1200\text{ K}$ , is reached on the timescale of 1–10  $\mu\text{s}$ , respectively, see Fig. 2(b). At temperatures  $T \geq \Theta$ , the particles are softened and establish significant adhesion contact with the substrate. The high temperature causes annealing (and annihilation) of deep traps [14] and discharging of the particles. Becoming neutral spheres, they move only slightly on the substrate due to Brownian motion until they collide with other particles and coalesce into chain-like clusters. At higher fluences significant discharging causes that the particles become immobile and mostly fixed on the silicon surface. The particle-particle and particle-substrate adhesion is increased due to surface softening/melting and the previously formed clusters are stabilized.

**4.3 Particle clustering** The number of particles  $N$ , connected into a chain-cluster strongly decreases with the particle diameter  $D$ , as shown in Fig. 2(c). It is clearly seen that particles with diameter of  $D = 90\text{ nm}$  tend to form very large chain(s) with  $N = 300\text{--}500$  nanoparticles in the spot. Extrapolation of the distribution curve to very large numbers indicates that  $N \rightarrow \infty$  is asymptotically reached for  $D \equiv D_0 \geq 60\text{ nm}$ . Fitting of the experimental results by:

$$N = AX^{-\alpha}e^{-\beta X} \quad (4)$$

where  $X = D/D_0$ ;  $D_0 = 60\text{ nm}$ ,  $\alpha = 3$ ,  $\beta = 0.2$ , and  $A = 2114$ , gives a very good agreement, see Fig. 2(c). This distribution called “power law distribution with an exponential cut-off” is a common alternative to the asymptotic power-law distribution, because it naturally captures finite size effects in the system of particles. In this distribution, the exponentially decaying term,  $\exp[-\beta(D/D_0)]$ , overwhelms the power-law behavior at very large values of  $X$ . This distribution does not scale and is thus not asymptotically a power law; however, it does approximately scale over a finite region before cut-off. The distribution can not scale as a power law in the limit  $X \rightarrow \infty$ , because the system is determined by the finite size of the particle diameter ( $D = D_{\text{max}}$ ), and also, the system has a finite (and not infinite) number of particles. The above distribution can be divided into: (i) The region, sensitive on  $D$  showing strong linear decrease of the chain length between  $D = 90\text{ nm}$  to about  $160\text{ nm}$ , (ii) The region, almost insensitive on  $D$  between  $D = 200\text{--}450\text{ nm}$ . In the future experiments, we are planning to test this distribution in a wider range of the particle diameters.

**5 Conclusions** The self-organization of nanoparticles induced by low energy ion irradiation is a complex phenomenon which breaks the 2D hexagonal lattice symmetry organization, and depends on both the particle charging and particle heating (surface melting). Both proc-

esses play a crucial role in the restructuring dynamics and depend on the particle size and on the ion fluence.

The strength of the Coulomb repulsion between the particles and the strength of the adhesion to the substrate and to the other particles may be responsible for different degree of reorganization of bigger and smaller nanospheres. At higher fluences, the particle discharging and the increased adhesion block further movement and reorganization of particles into chain-clusters. The average particle cluster size decreases with the increase of the particle diameter.

**Acknowledgements** We gratefully acknowledge the partial support from the croatian-hungarian bilateral agreement HR - 20/2008, the EU project ENIAC-JTI SE2A, and the János Bolyai Research Fellowship for the second author.

## References

- [1] T. van Dillen, A. van Blaaderen, and A. Polman, *Mater. Today* **7**, 40–46 (2004).
- [2] K. P. Velikov, T. van Dillen, A. Polman, and A. van Blaaderen, *Appl. Phys. Lett.* **81**, 838 (2002).
- [3] N. Nagy, A. E. Pap, A. Deák, E. Horváth, J. Volk, Z. Hórvölgyi, and I. Bársony, *Appl. Phys. Lett.* **89**, 063104 (2006).
- [4] Z. Zolnai, A. Deák, N. Nagy, A. L. Tóth, E. Kótai, and G. Battistig, *Nucl. Instrum. Methods B* **268**, 79 (2010).
- [5] T. van Dillen, E. Snoeks, W. W. Fukarek, C. M. van Kats, K. P. Velikov, A. van Blaaderen, and A. Polman, *Nucl. Instrum. Methods B* **175**, 350 (2001).
- [6] T. van Dillen, E. van der Giessen, P. R. Onck, and A. Polman, *Phys. Rev. B* **74**, 132103 (2006).
- [7] E. Snoeks, A. van Blaaderen, T. van Dillen, C. M. van Kats, M. L. Brongersma, and A. Polman, *Adv. Mater.* **12**, 1511 (2000).
- [8] E. Snoeks, A. van Blaaderen, T. van Dillen, C. M. van Kats, K. Velikov, M. L. Brongersma, and A. Polman, *Nucl. Instrum. Methods B* **178**, 62 (2001).
- [9] J. C. Cheang-Wong, U. Morales, E. Resendiz, A. Lopez-Suarez, and L. Rodriguez-Fernandez, *Nucl. Instrum. Methods B* **266**, 3162 (2008).
- [10] M. Skupinski, R. Sanz, and J. Jensen, *Nucl. Instrum. Methods B* **257**, 777–781 (2007).
- [11] M. Szekeres, O. Kamalin, R. A. Schoonheydt, K. Wostyn, K. Clays, A. Persoons, and I. Dékány, *J. Mater. Chem.* **12**, 3268–3274 (2002).
- [12] S. Yogev, J. Levin, M. Molotskii, A. Schwarzman, O. Avayu, and Y. Rosenwaks, *J. Appl. Phys.* **103**, 064107 (2008).
- [13] D. S. Grierson, E. E. Flater, and R. W. Carpick, *J. Adhesion Sci. Technol.* **19**, 291–311 (2005).
- [14] A. Stesmans, K. Clemer, and V. V. Afanas'ev, *Phys. Rev. B* **72**, 155335 (2005).